

# **Signal to Noise Improvements in Nuclear Magnetic Resonance Microcoils**

Robert Cooper

Dept. of Physics, University of Toledo, Toledo, OH 43606

Under the Direction of

Dr. Charles H. Pennington

Dept. of Physics, The Ohio State University, Columbus, OH 43210

Derek A. Seeber

Dept. of Physics, The Ohio State University, Columbus, OH 43210

Research supported in part by National Science Foundation – Research Experiences for  
Undergraduates.

## **Abstract**

In nuclear magnetic resonance (NMR), imaging at the cellular level is best attempted with NMR coils that approach the physical dimensions of the cell. A systematic procedure to test various design parameters on these coils was done to find the effect on the signal to noise ratio of water. The metal composing the microcoil was varied to test the effect of resistivity on signal to noise. Also, the leads connecting the coil to the circuit board were varied to find the effect on signal to noise. Intuition is correct that low resistance metals coupled with the least use of wire leads gives the highest signal to noise ratio.

# Introduction

## Basic NMR

Consider a nucleus and its proton and neutron constituents. Each proton and neutron has a spin  $1/2$  and contributes to the total spin of the nucleus. For the case of hydrogen with only one proton, its spin is  $1/2$ . As is normally done, this spin is associated with magnetic moment vector. The interactions of this nuclear magnetic moment with external fields is the essence of nuclear magnetic resonance (NMR).

Consider a spin oriented at an angle with an external magnetic field,  $H_0$ , that is in the  $+z$  direction. It can be shown that this magnetic moment will rotate around the magnetic field at frequency  $\omega$ . Where  $\omega_0$ , the Larmor frequency, is given as,

$$\omega = \gamma H_0, \quad (1)$$

where  $\gamma$  is a proportionality constant called the gyromagnetic ratio. For proton NMR  $\gamma = 42.576 \text{ MHz / T}$ . For field strengths of a few Tesla, the angular frequency is in the radio frequency. Figure 1 gives a visualization of the described situation.

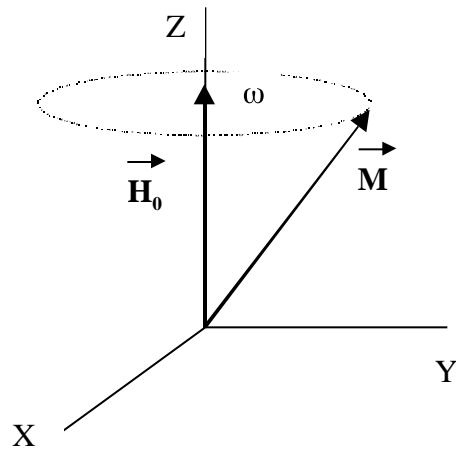


Figure 1: Magnetic moment in a magnetic field.

Often times a secondary field,  $H_1$ , is applied in the X-Y plane at the resonant Larmor frequency,  $\omega$ . This is essential to understanding how the X and Y components decay as the spins realign with the main field. To understand the effects of this  $H_1$  field, the main  $H_0$  field must be “subtracted.” This is done in the “rotating frame.”

If  $X', Y', Z'$  represent the rotating frame then  $Z, Z'$  coincide, but the  $X'-Y'$  plane rotates. The angular frequency of rotation is usually that of the Larmor frequency,  $\omega$ , but isn't required to be so. If the rotating frame rotates at  $\omega'$ , the effect is that the magnetic moment appears stationary. Thus, the effect of the main field,  $H_0$ , has been “subtracted.”

An interesting consequence is that application of external fields that are stationary in the rotating frame will also cause the magnetic moment to precess around this field (in the rotating frame). Hence, it is easy to see how a magnetic field could cause a moment lying along the Z (Z') axis to flip into the X-Y (X'-Y') plane. Such a pulse is called a 90° pulse. By sending a 90° pulse into the sample, a free induction decay signal is formed (see figure 2)<sup>1,2</sup>.

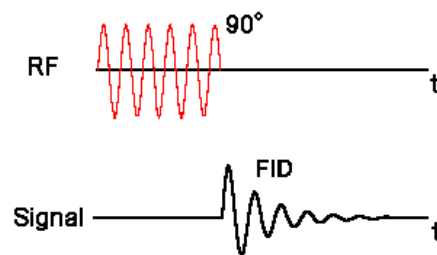


Figure 2: Pulse sequence and subsequent signal (FID – Free Induction Decay).

### Microcoils

A geometric argument for microcoils is given in Figure 3.

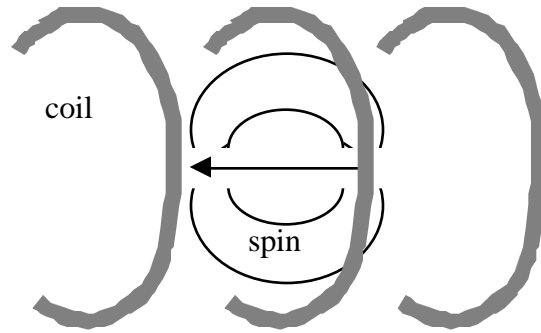


Figure 3: Microcoil arrangement with sample.

If the coil becomes too large, the field lines of a sample close upon themselves without crossing the coils. Without cutting lines, no EMF is induced in the coil. Obviously to image biological cells and their constituents, a microcoil must be on the order of a cells physical dimension. Microcoils typically have lengths  $\sim 330 \mu\text{m}$  and diameters  $\sim 100 \mu\text{m}$  giving volumes  $1 \times 10^{-12} \text{ m}^3$ ,<sup>3,4</sup>.

### **Signal to Noise Ratio**

In magnetic resonance imaging (MRI), the ability to resolve fine structures is directly linked to the signal to noise ratio (SNR). A SNR greater than unity implies the ability to differentiate a signal from the background noise. A SNR less than unity implies dominance of noise<sup>1,2</sup>.

To get a free induction decay signal, a 90° pulse is sent into the coil to excite the sample. The coil is then used to “listen” for the return pulse. This return pulse is a FID such as in figure 2. To get the proper time length for a 90° pulse, a range of pulse lengths is scanned. By picking the point with the largest signal, the pulse lengths are of various times are compared at that point. The signal at this point varies sinusoidally with pulse length (see figure 4). The average 90° pulse length is from 10 μs to 25 μs.

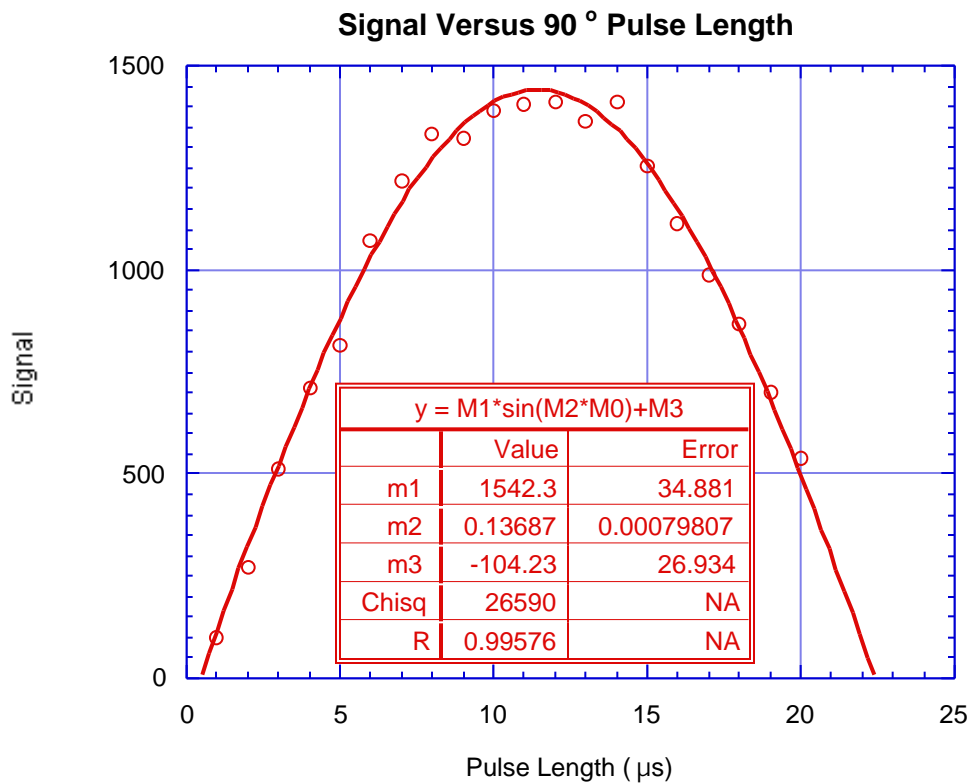


Figure 4: Signal varying as a sine curve as pulse length increases.

By taking the decaying signal (FID), the signal is defined as the largest part of the FID (usually within the first few microseconds). The noise is calculated as a RMS average of the signal many microseconds later. The ratio gives the signal to noise ratio (see figure 5). This SNR will be the basis for comparison throughout all changes in coil parameters.

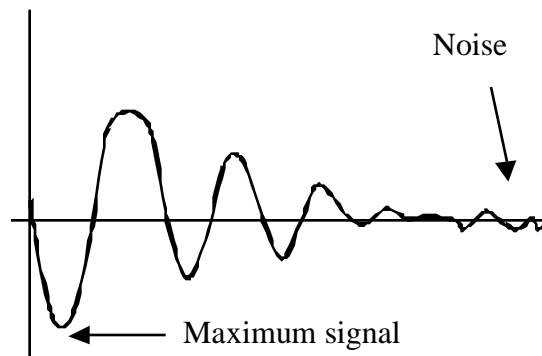


Figure 5: Visualization of signal to noise ratio in a FID.

## Experiment

### Resistive Wires

Noise in many electronic applications can effectively be modeled as Johnson noise. Johnson noise is proportional to the square root of the resistance of a component. By using various 25  $\mu\text{m}$  diameter, resistive wires to wind a microcoil, the SNR can be compared by changing these wires. Also, by winding with the same dimensions for each

coil, geometric factors are constant. This allows comparisons to the resistivity,  $\rho$ .

Hence, a theoretical estimate of SNR is given as<sup>5</sup>,

$$\frac{S}{N} \propto \frac{1}{\sqrt{R}}. \quad (2)$$

The geometry of each coil was a 5.5 turn coil. Spacing between the windings of the coil is twice that of the wire diameter. This reduces stray capacitance between the windings of the coils. This reduces the ac resistance. By winding in this manner with 25  $\mu\text{m}$  diameter wire, a coil of  $\sim 330 \mu\text{m}$  long and diameter of  $\sim 100 \mu\text{m}$  is formed. A detailed guide to winding these coils is given in Appendix A-C. The purpose is to verify the above formula, thereby justifying use of a low resistance wire such as copper.

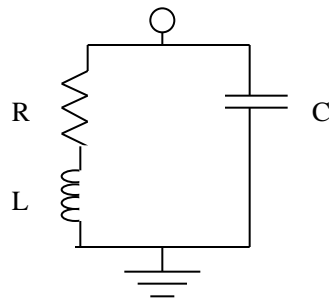
### **Lead Length**

A tuned microcoil is essentially a LC tank circuit tuned at the proton NMR frequency. It is well established that any length of free wire is an inductor. Hence, it is believed that shorter leads reduce stray inductance, thus improving SNR. The same coil was used and the long lead was shortened and the tuned again. This ensures the same coil geometry, isolating the inductance change to the lead length. Examination of the inductance versus lead length can be inferred by knowledge of the tuning capacitance.

## Discussion

### Resistive Wires

The capacitance required to tune each of the resistive wires was found to be smaller than the calculated value for a LC tank circuit. In fact, as resistivity increased, the required capacitance decreased. To account for the capacitance change, a RLC circuit (see figure 6) was modeled to account for the higher (potentially important) coil resistance.



Hence, the resistance can account for the drop in tuning capacitance from a LC tank circuit. To test the fit, the capacitance change was fit to the difference between a LC circuit and a RLC circuit. The equation of fit and resulting plot are given as (equation 4 and figure 7),

$$C_0 - C = \frac{C_0}{Q^2 + 1} = \frac{m_2}{m_1 \frac{1}{\rho^2} + 1} \text{ where } m_1 \text{ and } m_2 \text{ are fit parameters. (4)}$$

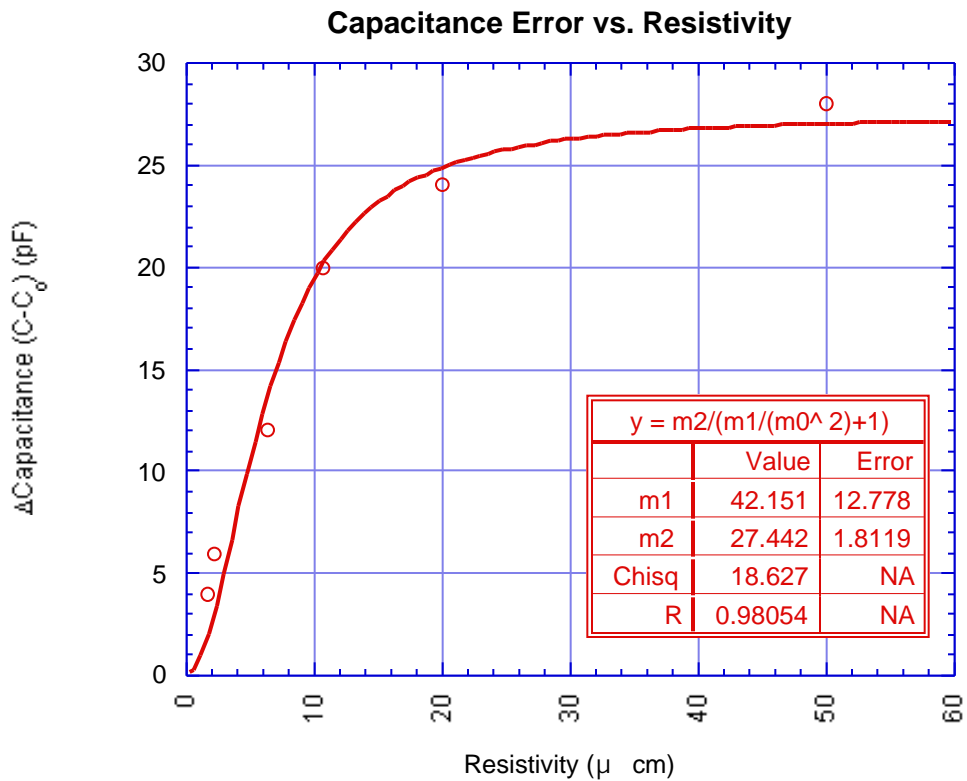


Figure 7: Capacitance error versus resistivity: plot and fit result.

Further verification of the RLC model is that inductance is a factor of the fit parameter  $m_1$ . A value of a few nanoHenries results. This is close to the geometrically calculated value. By plotting the SNR (per unit volume) versus resistivity on a log plot, a decrease is noticed. The log plot indicates a power of  $-0.83$  versus the expected  $-0.50$ . The possibility of added ac resistance effects could account for the disparity. Figure 8 shows the plot and fit.

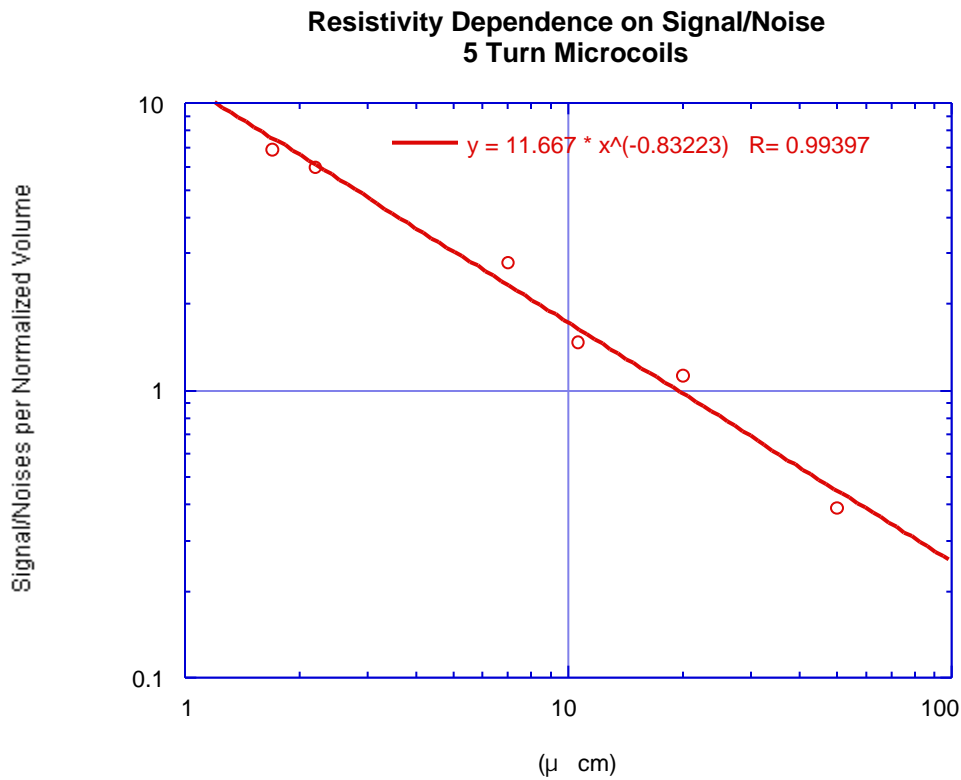


Figure 8: SNR versus resistivity on a log plot.

## Lead Length

By plotting the lead length and SNR, the SNR decreases, as expected, with the increase in lead length. By fitting to a power fit, the power of -.55 is rather close to -.50 (see figure 9). By examining Johnson noise, it is found that equation 2 is a specific case of <sup>5</sup>

$$\frac{S}{N} = \frac{1}{\sqrt{R}} \frac{1}{\sqrt{l}} \quad (5)$$

This is the case since copper is used throughout so the resistivity is a constant. To account for the “breakdown” observed in figure 8, it should be realized that the resistance change with copper leads is quite small when compared to the resistance range for the resistive wires.

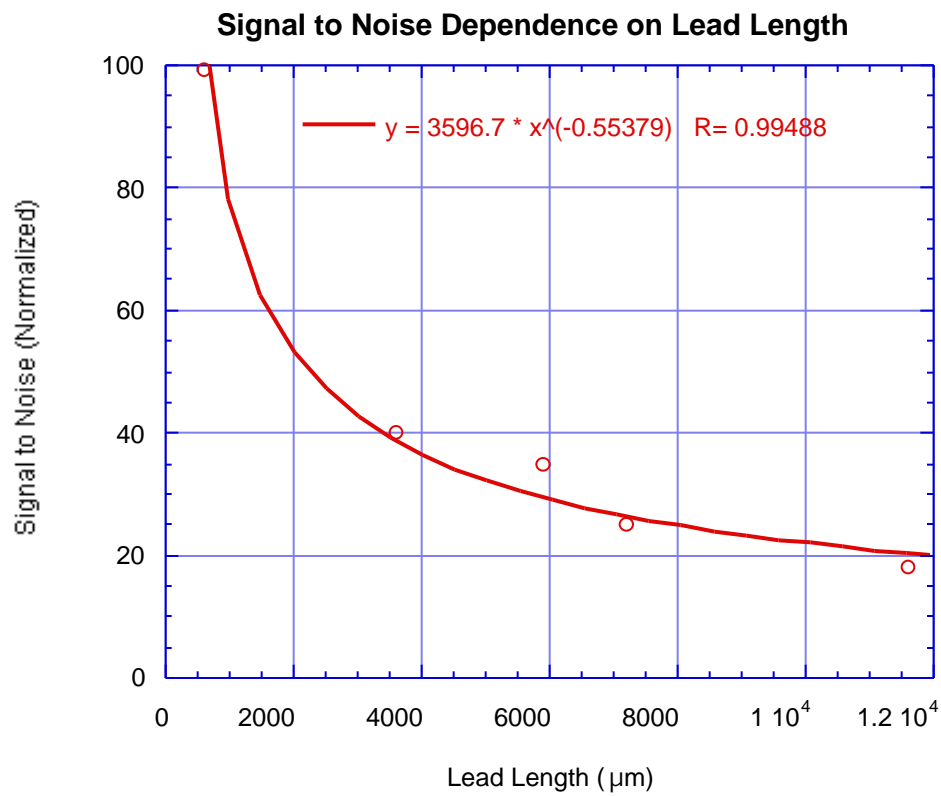


Figure 9: SNR versus lead length.

As leads are added, inductance and resistance (ac and dc) are added. By examination of equation 3, if the  $Q$  factor remains relatively constant or is large, the variation in tuning will be due to changes in  $L$ .

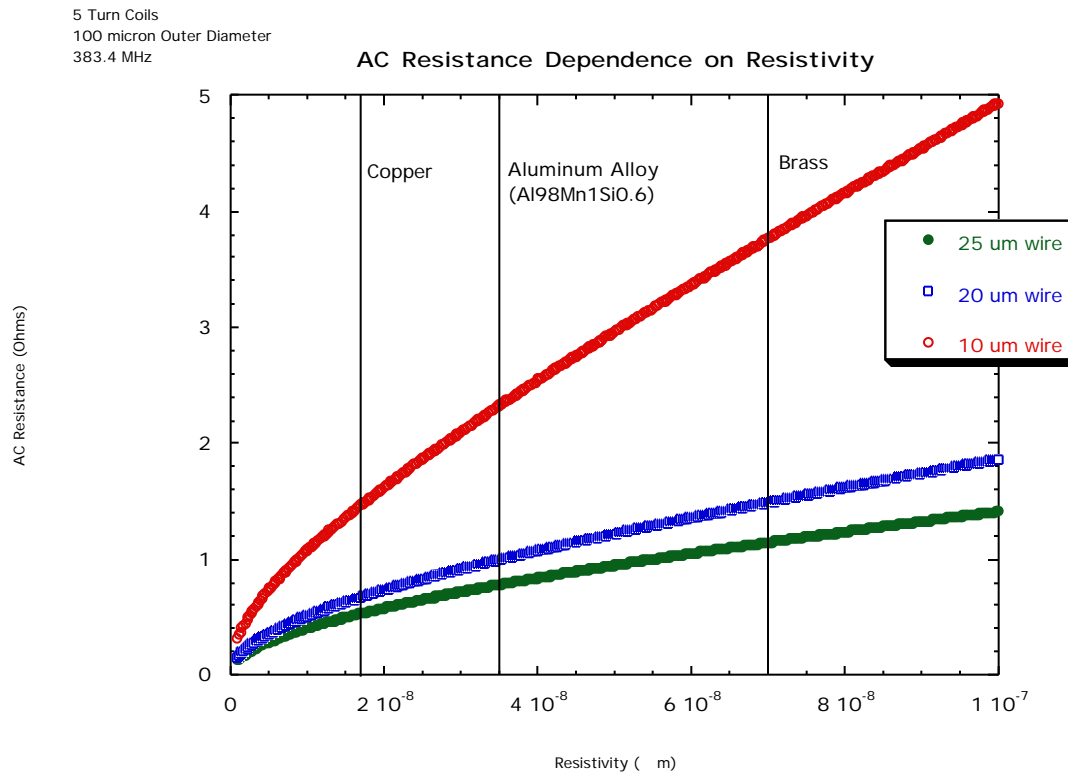


Figure 10: Graph of ac resistance (dominant) of a 5-turn coil.

A copper coil has an approximate resistance of 0.5 (see figure 10)<sup>6-9</sup>. The resistance in the leads (ac and dc) is linear in lead length. The inductance in the coil is approximately 2.2 nH. This value was calculated from geometrical factors. The inductance of the leads can be estimated to be,

$$L = k\ell \ln \frac{2\ell}{a} - .75 . \quad (7)$$

Where  $k$  is a constant,  $a$  is the radius of the wire, .75 comes from ac skin depth effects from low frequency (it will be somewhat higher at NMR frequencies), and  $\ell$  is the length of the lead<sup>5</sup>. Within the range of the lead lengths tested, the inductance is approximately linear. Hence,  $Q$  given as,

$$Q = \frac{\omega L}{R} = (2\pi \cdot 383 \text{ MHz}) \frac{(2.2 \times 10^{-9} \text{ H} + 1.2 \times 10^6 \text{ H/m } \ell)}{(.5 + 4 \frac{1.68 \times 10^{-8} \text{ m}}{\pi(12.5 \times 10^{-6} \text{ m})^2} \ell)}. \quad (8)$$

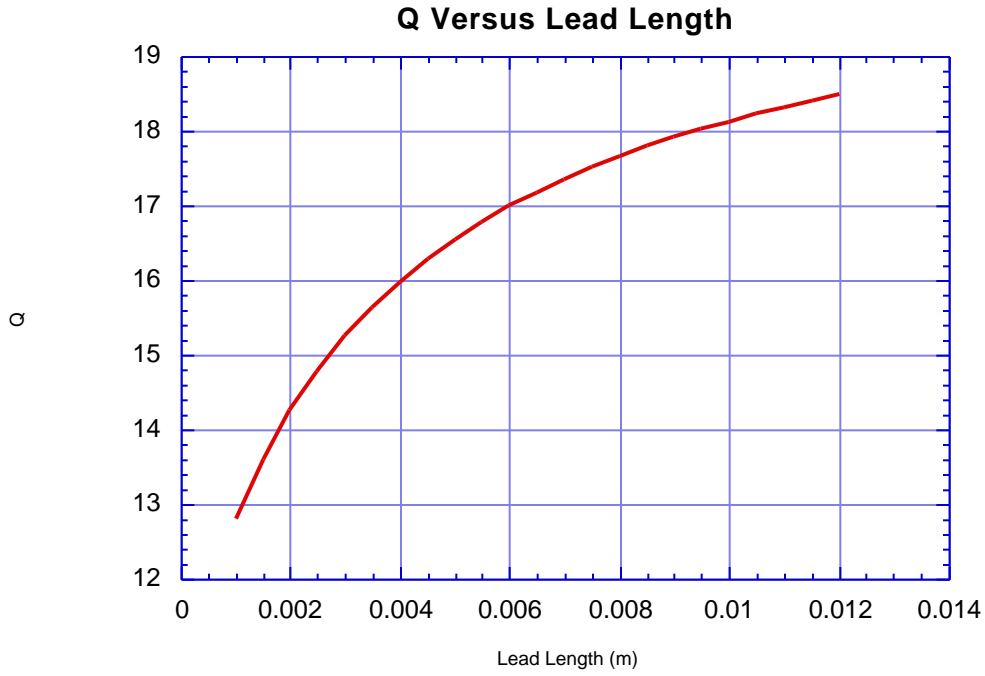


Figure 11: Q factor versus lead length.

The plot of equation 8 is given in figure 11. It can be seen that when  $Q$  is input into equation 3, that its effect on tuning capacitance is negligible. Hence, the tuning capacitance is almost entirely effected by the  $C_0$  term and is approximately,

$$C = k C_0 = k \frac{1}{L} \text{ where } k \text{ and } k \text{ are constants.} \quad (9)$$

Assuming that the total inductance is approximately linear for the leads and constant in the coil, the fit for the tuning capacitance becomes (see figure 12),

$$C = \frac{1}{\omega^2 L} = \frac{1}{m_1 + m_2 \ell} \text{ where } m_1 \text{ and } m_2 \text{ are fit parameters.} \quad (10)$$

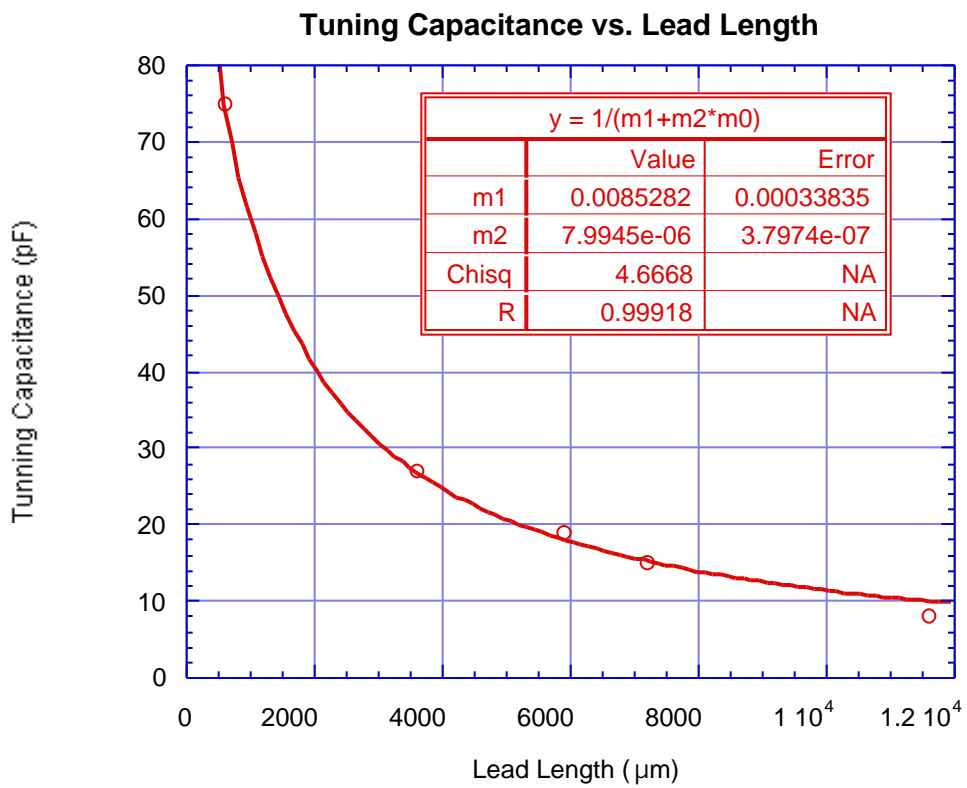


Figure 12: Capacitance versus lead length with fit (equation 9).

The fit parameters are factors of coil inductance and inductance per unit length of leads. By dividing out these factors, reasonable values for the inductance of the coil (~1.5 nH) and inductance per unit length (~1.4 nH / mm) are left. This further asserts the validity of the approximations.

## Conclusions

A systematic approach to verifying seemingly intuitive concepts was performed. Intuitively, it is expected that low resistivities will yield the highest signal to noise ratio. Testing of various metals of known resistivities and consistently winding the same geometry allowed verification of this fact. In fact, the breakdown of the LC tank circuit was found in this test. A more general RLC circuit was required to fully explain the tuning capacitance. The explanation has an elegant form allowing it to be applied to more complicated problems.

By changing the lead length and assuming relatively long leads, a simple formulation predicts the tuning capacitance. Though both the resistance and inductance change with each lead, the effects are offset in the quality factor, leaving the original capacitance from the LC circuit as the sole source of change. Also, because inductance doesn't directly contribute to the noise factor, signal to noise was found to obey a relatively simple formula in equation 5.

Overall, intuition is correct in predicting qualitatively that low resistivities and short connecting leads will give higher a SNR. Intuition does not explain the effects of tuning on these circuits. Without a properly tuned circuit, no NMR can be performed.

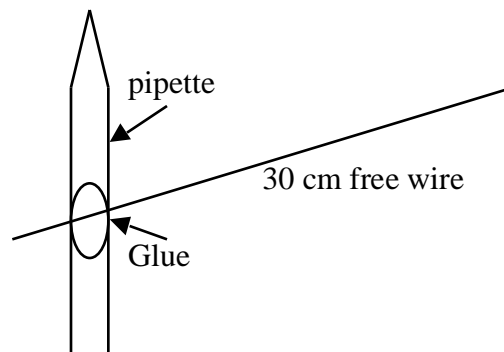
## **Acknowledgments**

I wish to acknowledge my advisor Charles Pennington, graduate student Derek Seeber , and electronics shop director John Hoftiezer for the help that each gave. Recognition goes to the NSF for giving me the opportunity to research at The Ohio State University.

## APPENDIX A: Winding Procedure for a Nuclear Magnetic Resonance Microcoil

Step A1: To wind coils of some definite diameter, a micropipette puller is used. The pulled pipette has a tapered end and by inspection under a microscope, the proper diameter can be found. In our case, the microcoil diameter is 100  $\mu\text{m}$ . This is achieved with quartz glass capillary tubes from Sutter Instruments (CAT# Q100-70-10). The capillary tubes have an outer diameter of 1.0 mm, inner diameter of .70 mm, and are 10 cm in length. Program 81 of the Sutter Instruments P-2000 pipette puller was employed (Heat = 840, Fil = 5, Vel = 50, Dell = 120, Pull = 175).

Step A2: Once a pipette has been made, the coil wire is to be attached. Attachment at the center of the pipette is accomplished with Norland Optical #68. The advantage is that it cures under UV light allowing manipulation before drying. Allow approximately 30 cm for winding (see figure A1). Cure under UV light for 5 minutes.



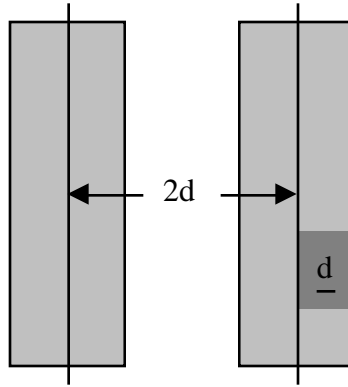


Figure A2: Wire spacing

Twenty turns of the translation knob gives one inch of translation. This is coupled to 5:1 gear, and the remaining gear ratio can be selected from Table 1 to give the proper spacing. Equation A1 describes Table A1 below,

$$\text{Wire Spacing} = \frac{25.4 \text{ mm}}{20 \cdot 5 \cdot G}, \quad (\text{A1})$$

where  $G$  is the added gear ratio. Table A1 calculates the wire spacing given a large and small gear.

Large Gear (groove #)	Small Gear (groove #)	
	10 Grooves	12 Grooves
25	102	121.9
36	71	84.7
44	58	69.3
48	53	63.5
60	42	50.8
72	35	42
80	32	38
90	28	34
100	25	30
120	21	25
130	19.5	23

Table A1: Wire spacing ( $\mu\text{m}$ ).

These gears will be installed on the drill chuck side. The small gear is attached to the drill chuck axle, and the large gear on the translation screw axle.

Step A4: Fasten large end of pipette into drill chuck. The wire should be hanging out onto the table. Place rectangular piece with set screws facing towards the drill chuck onto the winding apparatus (see figure A3).

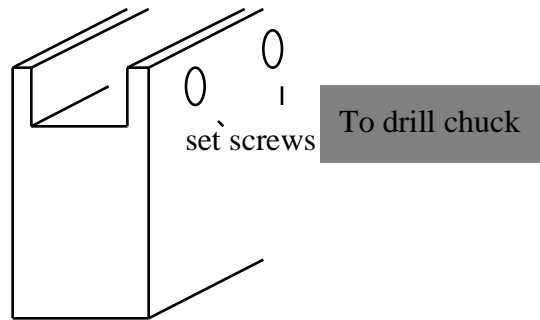
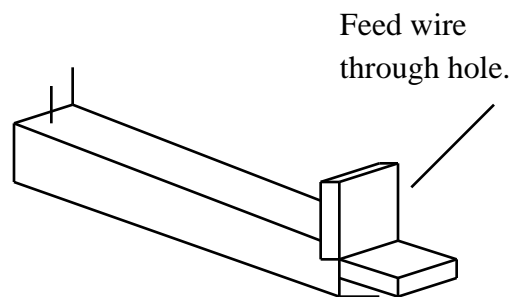


Figure A3: Piece orientation and description.

Step A5: Thread the wire into the long rectangular piece (see figure A4). Proper lighting will help. This rectangular piece fits into the above-mentioned piece from figure A3. It is fastened in place by the above-mentioned set screws.



wound coil. Note that the set screw on the bottom of the drill chuck knob should be loosened as well.

Once the wire has reached the field of view, the rectangular piece in figure A4 should be moved as close as possible (not touching) to the pipette. The horizontal nut at the bottom raises and lowers, and the linear translation moves left and right. The wire should be perpendicular to pipette. The linear translation should be rotated until it starts to move. This takes up the “slop” in the machining.

Step A7: A belt is attached to the two gears, and the set screw at the inside-bottom of the stand is tightened to prevent the large gear from moving around the curved slot. By turning either of the knobs (in the same direction as before), the coil will begin to wind. Wind until a coil of  $n$ -turns of proper diameter is formed. Apply glue on only the  $n$ -turns of the coil. Cure under UV light for 3 to 4 minutes.

Step A8: Cut the wire on the rectangular piece of figure A4. Leave about 1 or 2 cm from the coil. Remove the rectangular piece of figure A4 and the belt. Cut the wire close to the large glue spot of step 2. Unwind by holding wire (closest the glue spot) and turning the drill chuck knob “away” again. Unwind until desired turns. Cut the lead to about 1 or 2 cm or as desired. A 4.5 turn coil should look similar to figure A5.

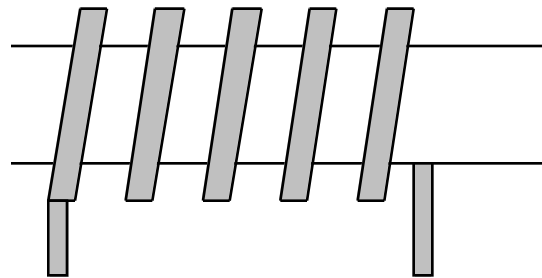


Figure A5: Coil.

Step A9: Turn coil until leads face horizontal and away. Tighten set screw under drill chuck knob. Cut a small amount of the tip after the coil. Attach a prepared board (Appendix B) to the piece similar to the piece in figure A3. The SMA should be facing “inward,” thus the substrate side is facing out (see figure A6).

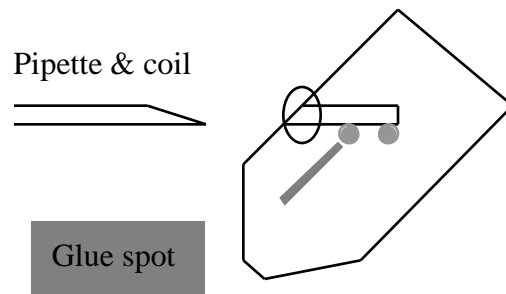


Figure A6: Orientation of board.

Step A10: Using the nut on the bottom, linear translation and the screw along the back of the mounting piece, place the pipette and coil into the slot on the board. The pipette should rest along the bottom of the chip, be pressed as close to the contact pads (still within the groove), and have the coil between the contact pads. Once in place, thoroughly glue the pipette in place (see figure A6). Cure with UV.

Step A11: Remove board from mounting piece. Cut remaining pipette being sure to leave about 1 cm (to fill). If any glue spot remains on pipette, scratch it off.

Step A12: Fold leads into nearest solder pads. It works best to bury the lead somewhat taut into the solder. “Tin” the iron with indium low temperature solder and put a small amount sticking from the iron tip. Heat the solder and watch that the leads don’t eject themselves. Run a continuity test to be sure of proper solder. Calculate the approximate capacitance for tuning and tune (see Appendix C). Put the capacitor as far from the coil as possible. Push some solder around the ends of the capacitor, apply solder. The pad that is connected by the button, will again take longer. Watch that the leads do not eject from the liquid solder. The approximate capacitance used is 10 pF -100 pF.

## **APPENDIX B: Preparing Circuit Board**

Step B1: Insert the copper plug into center hole on the circuit board such that the larger flat end is on the copper ground side of the board. Apply flux and apply a generous amount of solder around the plug.

Step B2: Insert the SMA such that the connector is facing upward from the non-copper substrate side. Flux the three sides not on the end and solder along these ends. Apply flux and solder around the center pin and track. Do not let the solder touch the outer four pins.

Step B3: Flux both pads closest to the groove. Apply low temperature indium solder to both pads. Do not let it bridge. Use knife to scrape flat both pads. This will leave a soldered pad to put wires and capacitors.

Step B4: If a matching capacitor is required, take a knife and thoroughly cut a gap in the main trace 5 mm from the groove. This will allow a matching capacitor to be soldered across. Put solder on both sides and cut flat. Again, prevent bridging.

## APPENDIX C: Tuning the Coil

Step C1: From Wavetek Model 1092, connect the scope out plugs from VERT to Y and HORIZ to X on an oscilloscope. Place scope in X-Y mode.

Step C2: Find the IN / OUT / CPL 3-plug box. The board goes to the IN plug. The OUT goes to the Wavetek RF OUT plug. The CPL plug goes to the Wavetek DETECTOR IN.

Step C3: Turn on the Wavetek and oscilloscope. Set the attenuation to 10 dB, switch to RECUR, and put the SWEEP WIDTH at its highest.

Step C4: On the back of the Wavetek, plug the EXT MARKER into the 383 MHz generator.

Step C5: On oscilloscope, find the curves. Switch on the 383 Mhz generator to locate the tuning frequency. Attach the circuit and find the peak.

Step C6: If the peak is too high, add capacitance. If the peak is too low, drop capacitance. This follows from,

$$\omega = \frac{1}{\sqrt{LC}}.$$

# Bibliography

- 1 E. Fukushima and S. B. Roeder, *Experimental Pulse NMR: A Nuts and Bolts Approach* (Addison-Wesley, Reading, MA, 1981).
- 2 C. P. Slichter, *Principles of Magnetic Resonance* (Springer, New York, 1996).
- 3 D. A. Seeber and J. H. Hoftiezer and C. H. Pennington, *The Review of Scientific Instruments* **71**, 2908-2913 (2000).
- 4 D. A. Seeber and J. H. Hoftiezer and W. B. Daniel and M. A. Rutgers and C. H. Pennington, *Review of Scientific Instruments* (2000).
- 5 D. Summer, *The ARRL UHF/Microwave Experimenter's Manual* (The American Radio Relay League, Newington, 1990).
- 6 S. Butterworth, *The Wireless Engineer* **3**, 203-210 (1926).
- 7 S. Butterworth, *The Wireless Engineer* **3**, 309-316 (1926).
- 8 S. Butterworth, *The Wireless Engineer* **3**, 417-424 (1926).
- 9 S. Butterworth, *The Wireless Engineer* **3**, 483-492 (1926).